COMPUTER SIMULATION OF A NEW METHOD TO DRY LUMBER USING SOLAR ENERGY AND ABSORPTION REFRIGERATION

Wayne A. Helmer

Associate Professor
Department of Mechanical Engineering and Energy Processes, Southern Illinois University
Carbondale, IL 62901

and

Peter Y. S. Chen

Forest Products Technologist
North Central Forest Experiment Station, U.S. Department of Agriculture–Forest Service
Carbondale, IL 62901

(Received February 1984)

ABSTRACT

A mathematical model for a solar-absorption dehumidification lumber dryer has been developed. Performance of a commercial size lumber kiln of 60 m^3 (25,000 board-feet) was simulated for a southern Illinois climate for four different seasons of the year. The solar-absorption system dried yellow-poplar lumber as fast as a conventional vapor-compression dehumidification system while reducing the electrical energy costs by 85%. Capital costs and yearly fuel costs were compared to an oil-fired boiler system, a wood-fired boiler system, and a vapor-compression lumber-drying system.

Keywords: Solar energy, lumber drying, absorption refrigeration, dehumidification drying, economic analysis.

INTRODUCTION

Approximately 40% of the total yearly United States energy supply is consumed by the industrial sector. This amounts to about 32×10^{15} kJ (Auer 1980) per year, of which almost 10×10^{14} kJ (6%) is consumed by the United States forest industries (Comstock 1975). Since 60% to 70% of the energy consumed in manufacturing wood products occurs during drying, many new drying processes are under study to reduce the energy required for furniture and lumber manufacturing.

Dehumidification drying is one new method that is currently receiving much attention by the forest products industry. Many new lumber drying plants are installing dehumidification units in their dry kilns because of the reduced capital costs for these systems. Figure 1 illustrates the basic components of a vapor-compression dehumidification kiln. Heat is added to the moist air in the kiln by the condenser, which drives the moisture from the wood. Energy from the moist air is recovered in the evaporator where the water vapor is condensed out of the air on the cold heat exchanger surfaces. Dehumidification drying has the advantage that the energy in the moist air is not lost to the environment, as occurs during venting of a steam-heated kiln. Also, the electrical energy used to drive the compressor is more efficiently utilized than the energy supplied to a conventional steam-heated kiln. Here, the sum of the useful energy effects in the condenser and

Wood and Fiber Science, 17(4), 1985, pp. 464–476

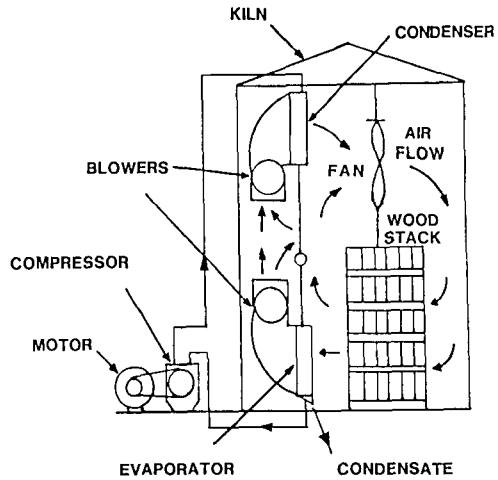

FIG. 1. Vapor-compression dehumidification lumber kiln.

dehumidifying coil is at least twice the value of the electrical energy input to the compressor motor.

However, even though overall energy consumption is reduced in a dehumidification dryer, the net operating cost can be equivalent to a conventional steam-heated kiln because the vapor-compression dehumidifier uses expensive electrical energy to operate the system. If the dehumidification unit could be powered by solar energy, there would be a great potential for a large reduction in the energy costs. Solar energy has been used in many residential and commercial demonstration projects with successful technical performance using absorption chillers. Figure 2 is a schematic of a solar-powered absorption unit that dehumidifies the moist air in a lumber-drying system.

The goal of this paper was to develop an analytical model capable of being used to simulate the performance of a solar-powered absorption system for drying lumber in a commercial kiln and to compare its performance to conventional drying systems. Energy consumption, drying rate, operating costs, and capital investment for this drying system are compared to a vapor-compression dehumidification lumber-drying system and conventional drying systems.

MODEL DEVELOPMENT

System description

The solar-absorption dry kiln shown in Fig. 2 dries the lumber on a batch basis very similar to that done in a dehumidification kiln. Here an array of liquid heated collectors are used to supply hot water to the hot storage tank. This stored energy provides heat to activate the generator in the absorption system. With the absorption unit operating, heat is extracted from the cold storage tank, and heat from the absorption condenser is discharged to the ambient air in a wet cooling tower. Chill storage water is circulated to a dehumidifying coil in the kiln to remove moisture from air in the drying chamber.

The drying of wood is accomplished by the hot kiln air passing through the wood stack and receiving moisture from the wood. The moist air passes through

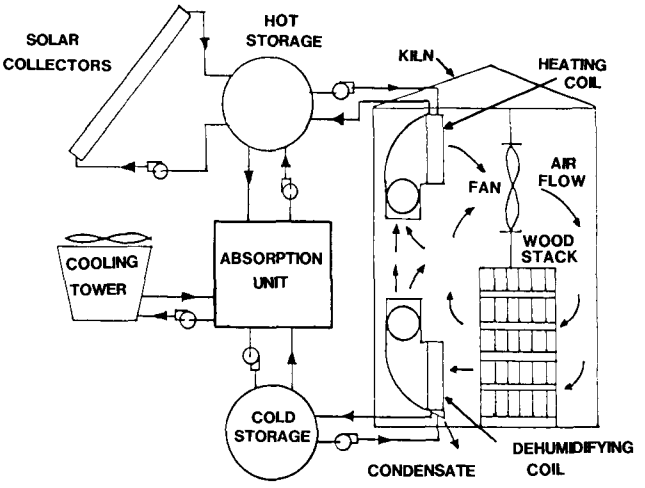

FIG. 2. Solar-absorption dehumidification lumber kiln.

the dehumidifying coil where water vapor is removed, after which the cool air is circulated through and heated up by the heating coil that is heated by the water from the hot storage tank.

Kiln and wood characteristics

The analysis of the kiln envelope, moist air, and wood stack has been well documented previously (Helmer et al. 1980, 1982). Therefore, model development is only summarized here.

A one-dimensional transient analysis of the energy flow in the moist air and green wood, together with a mass balance on the moist air in the kiln, yield two nonlinear ordinary differential equations, which can easily be solved numerically with the aid of a computer. The resulting equations predict air dry bulb temperature and air humidity ratio as a function of the ambient dry bulb temperature, wood drying rate, heat input from the hot storage tank, heat removal by the cooling coil, as well as specified input information on the dryer system configuration and wood type. The wood drying rate is assumed to be directly proportional to the humidity ratio difference between the wood surface and the moist air, and inversely proportional to the wood drying resistance (Bramhall 1976). Initial kiln and wood conditions are listed in Table 1.

TABLE 1. *Initial kiln and wood conditions and other independent variables.*

60 m^3 (25,000 board feet) yellow-poplar lumber of 2.54 cm thickness
92% initial wood moisture content
4,000 m^2 liquid solar collector area
205 m^3 storage tanks
300 m^3 drying chamber
0.75 kw circulation fans (total of five)
264 kJ/s LiBr-H_2O absorption chiller

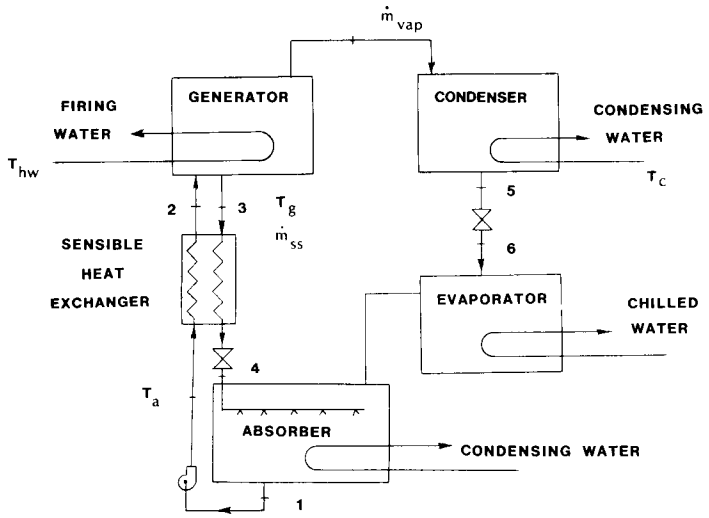

FIG. 3. Single effect lithium bromide-water absorption chiller.

Absorption machine

In absorption systems, a heat input is used to cause the cooling effect, in contrast to the compressor work input in a vapor-compression refrigeration system. Figure 3 illustrates the basic components in a lithium bromide-water (LiBr-H_2O) system. In the generator, heat from the solar collectors boils the water from the lithium bromide-water solution. Heat is rejected and the water vapor is condensed in the condenser. The pressure is dropped as the water passes through a control valve and on into the evaporator. In the evaporator the water boils at a low temperature to provide cooling of the chilled water circulated from the cold water storage.

The strong solution leaving the generator passes through a heat exchanger, where this solution is cooled and the weak solution from the absorber is preheated. In the absorber, the strong solution from the generator is mixed with water vapor from the evaporator. The resulting weak solution is pumped back into the generator. The heat of mixing produced in the absorber is transported to a low-temperature source. Typically, this low-temperature source for the absorber and the condenser is return water from a cooling tower.

The advantage of an absorption machine is that liquid is pumped versus a vapor compressed in a vapor-compression refrigeration system, thereby requiring less mechanical energy to move the working fluid through the system components. The pumping power required to move a liquid is usually much less than that necessary to move a gas through the same system.

There are many absorption machine models in the literature. However, most of these are for steady-state operation (Bogart 1982; Auh 1977; Allen and Morse 1976), and only a few include the transient start-up and cool-down period (Anand 1982; Auh 1979; Guertin and Wood 1980). The transient period must be included in the absorption chiller analysis since chiller cycling can significantly reduce the overall cooling capacity. Several investigators have modeled chiller transients

using complete heat and mass transfer equations as well as thermodynamic relationships. While this method can provide close correlation between experiment and theory, extensive computer time is consumed through the solution of the numerous equations. The simpler approach used in this study provides adequate simulation of the steady-state and transient operation of the absorption machine.

Blinn et al. (1979) used a lumped capacity model for an LiBr-H_2O chiller utilizing different time constants for start-up and shut-down, i.e.,

$$\tau_h = 0.133 \text{ h} \quad \text{and} \quad \tau_c = 1.05 \text{ h}$$

Their model was used in the present simulation to predict the performance of the absorption unit in the dehumidification dryer. During the start-up and cool-down period, the generator temperature was calculated during any time step from

$$T_{g,h} = T_{g,ss} + (T_{g,0} - T_{g,ss})\exp[-(t - t_0)/\tau_h] \tag{1}$$

and

$$T_{g,c} = T_a + (T_{g,0} - T_a)\exp[-(t - t_0)/\tau_c] \tag{2}$$

The instantaneous heat rate to the generator and cooling capacity of the evaporator were then given by

$$q_{gen} = f_1(T_g, T_c) \tag{3}$$

$$q_{cool} = f_2(T_g, T_c) \tag{4}$$

where f_1 and f_2 are curve fits of manufacturer's experimental performance data.

Cold energy storage tanks have been shown to reduce chiller cycling and thus increase overall cooling capacity. The hot and cold storage tanks were assumed to be spherical in shape. Heat loss or gain to the ambient air was calculated using the overall wall heat transfer coefficient (0.19 $W/m^2 - °C$) and assuming that the water was well mixed at a uniform temperature. An energy balance on the hot and cold storage systems yielded

$$C_h dT_{hs}/dt = q_1 - q_h - q_{gen} \tag{5}$$

where

$$q_1 = \eta I A_1 \tag{6}$$

$$q_{hc} = U_h A_h (T_{hs} - T_a) \tag{7}$$

and

$$C_c dT_{cs}/dt = q_c + q_d - q_{cool} \tag{8}$$

where

$$q_c = U_c A_c (T_a - T_{cs}) \tag{9}$$

The cooling tower was modeled by assuming that the cooling water returning to the absorption machine was delivered at a given increment above the ambient wet bulb temperature. For the present chiller this yielded,

$$T_c = T_{wb} + 5.5 \tag{10}$$

TABLE 2. *Dehumidifying coil parameters.*

1.89 kg/s air flow rate	3.15 aluminum fins per cm
2.02 kg/s water flow rate	15.2 cm deep
0.464 m^2 frontal area	1.27 cm water tube diameter
0.071 m^3 heat exchanger volume	

Heating and dehumidifying coil

Calculation of the water removal rate in the dehumidifying coil was determined using the method suggested by ASHRAE (Anonymous 1979). In this technique, the point on the air-side where the surface temperature reaches the moist air dew point temperature is determined using the coil characteristic. The coil characteristic is a function of the air and water heat transfer coefficients, fin area, tube area, and metal conductivities. With this information, the kiln air conditions and the chill water temperature, the wet and dry surface areas can be calculated, which determine the sensible and latent loads as well as the water removal rate. The specific conditions used to simulate the dehumidifying coil are listed in Table 2, and they are typical of the geometry and operating conditions used in cooling coils for this size of system. Table 3 lists the characteristics of the hot water heating coil.

Collectors

The solar collectors were modeled using performance data in terms of efficiency equations for the specific type of collector selected,

$$\eta = F(\tau\alpha) - FU_c(T_i - T_a) \tag{11}$$

Table 4 lists the parameters selected for the evacuated-tube collector assumed. The liquid collectors were assumed to drain back to storage on off-cycle so there was no need to simulate a heat exchanger in the hot storage tank or an antifreeze solution in the collectors.

Parasitic power is required to move heat transfer fluids through the system components. Fan and pump energy consumptions were calculated using the basic equation (Lunde 1980).

$$E = \frac{\dot{m}\Delta h \rho_w}{\rho \eta_m} \Delta t$$

Fan pressure drop per row was assumed to be 0.102 cm − H_2O per row. The motor efficiency for all of the fans and pumps can vary significantly depending on the manufacturer's quality; however, a reasonable value of 0.65 was assumed for all motors. Collector water pressure drop data were taken from manufacturer's

TABLE 3. *Heating coil parameters.*

24.9 kg/s air flow rate	3.15 aluminum fins per cm
2.02 kg/s water flow rate	26.8 cm deep
9.29 m^2 frontal area	1.27 cm water tube diameter
2.49 m^3 heat exchanger volume	0.102 cm − H_2O/row pressure drop

TABLE 4. *Solar collector performance parameters and operating conditions.*

Type	Evacuated-tube
Surface area (m^2)	2,323
Flow rate ($1/s\text{-}m^2$)	0.015
F ($\tau\alpha$)	0.600
F U_c ($W/m^2\text{-}°C$)	0.901
Tilt angle	latitude + 15 deg
Reflector	yes

information (Anonymous 1980). The pressure drop through the generator, evaporator, and the condenser in the absorption unit was scaled up assuming the basic performance of an Arkla 3-ton chiller (Anonymous 1976).

Weather data

Climatic radiation data were taken from SOLMET data (Cinquemani et al. 1978) using monthly average values from Evansville, Indiana. Hourly average values were calculated using the method developed by Liu and Jordan (1977). Dry bulb data were extracted from Typical Meterological Year (TMY) data from the National Climatic Center, Asheville, North Carolina. Wet bulb temperatures were calculated using wet bulb temperature bin data. Four seasons of the year were modeled for the months of January, April, July, and October to provide seasonal performance of the solar drying system. A summary of the monthly average total hemispherical solar radiation is given below:

Month	January	April	July	October
Average insolation ($MJ/m^2\text{-}day$)	6.52	17.03	21.80	12.34

Control

The control of the complete drying system was accomplished in the following manner. Whenever the solar radiation was sufficient to raise the outlet temperature of the liquid collectors 3 C above the storage temperature, the collector pumps would operate. The pumps would stop when the temperature difference reached 1.5 C. The absorption unit would operate whenever the hot storage was greater than 77 C and whenever the cold storage was greater than 13 C. Chill water from cold storage was circulated through the dehumidifying coil whenever the kiln air relative humidity was above a set value determined by the wood moisture content (Helmer et al. 1980). Hot storage water was circulated through the heating coil whenever it was required in order to keep the dry bulb temperature at the level required by yellow-poplar drying schedule (Rasmussen 1961).

SIMULATION RESULTS

The drying performance results are presented in Figs. 4 through 6 for the month of October; however, these results are typical for the other months as well. The kiln dry bulb temperature is kept around 66 C for about the first 2 days; thereafter the temperature stays in the range of 55 C to 65 C. The kiln relative humidity remains fairly constant, around 80%, until the moisture content of wood reaches about 40% (about 3½ days). From then on the kiln relative humidity decreases

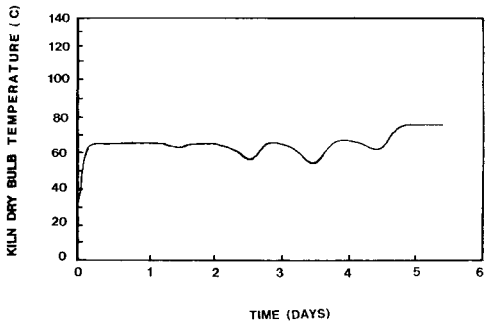

FIG. 4. Kiln dry bulb temperature during solar-absorption dehumidification drying of 2.54 cm yellow-poplar lumber.

gradually to a value of 25%. It takes 5½ days to dry the lumber to 8% moisture content. The hot and cold storage tanks enabled dehumidification and heating continuously throughout the drying process, thus eliminating the daily fluctuating dry bulb and wet bulb temperatures and moisture content experienced in a purely solar heated dry kiln (Helmer et al. 1982). Because of this better environmental control, wood quality probably would be enhanced compared to solar drying alone (Rosen 1982).

Drying times and energy consumption for the solar-absorption dryer are presented in Table 5. The drying times for the various months really did not vary that much. The tilt angle (latitude plus 15 degrees) enabled greater solar insolation utilization in January when it is needed more. A conventional steam-fired kiln will dry the same yellow-poplar lumber in about 6–10 days, which includes time for conditioning (one day or less). Therefore, the solar-absorption drying system is able to dry lumber at a rate equal to or faster than a conventional steam kiln.

Table 5 indicates that the fan energy is about equally divided among the different units. The pump energy is mainly consumed by the solar collectors with only about 13% of the pump energy consumed by the absorption unit pumps. The fans consume about 40% of the total electrical energy with the pumps consuming the remainder. The average specific energy consumption is 0.123 kwh/kg based on an average of 24,102 kg of water removed from the wood.

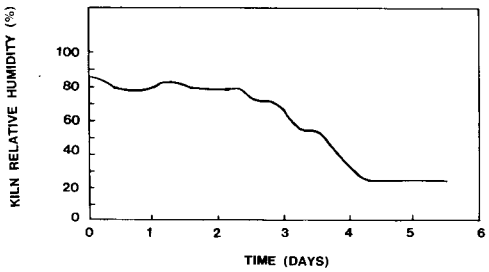

FIG. 5. Kiln relative humidity during solar-absorption dehumidification drying of 2.54 cm yellow-poplar lumber.

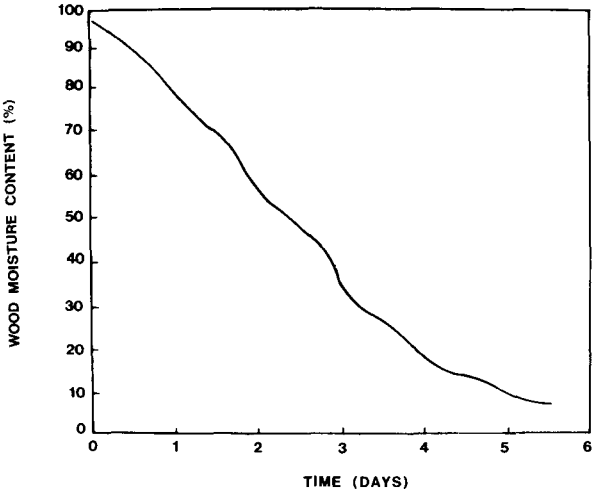

FIG. 6. Drying curve for solar-absorption dehumdification drying of 2.54 cm yellow-poplar lumber.

ECONOMIC EVALUATION

The solar-absorption dryer was compared to three other drying systems for energy consumption, capital cost, and fuel cost. The three systems examined were: a wood-waste fired boiler (indirect dryer), an oil-fired kiln, and a vapor-compression dehumidifier. For all systems, it was assumed that 45 charges of 60 m^3 (25,000 board-feet) of 2.54-cm-thick yellow-poplar lumber were dried yearly. A drying efficiency of 50% was assumed for the wood and oil-fired kilns. The cost of the basic kiln structure is not included in the costs that are presented below.

The wood-waste boiler capital cost was estimated at $33.2 per kg of steam produced, based upon quotes obtained from several boiler companies. This capital cost included the cost of the boiler, wood stoker, smoke stack, wood storage, and handling system. A boiler efficiency of 65% was assumed in burning 50% moisture content (oven-dry) wood at 9,864 kJ/kg (4,250 BTU/pound) of wet wood. A 9,090 kg-steam/h capacity boiler was assumed. Wood chips are available locally at $14.3/$10^3$ kg ($13/ton) and were assumed in the present analysis.

The oil-fired boiler was assumed to burn fuel oil at 40,190 kJ/liter (144,000 BTU/gal) having a boiler efficiency of 83%. The capital cost was evaluated from Curtis (1982).

The dehumidifier energy consumption data were taken from Eggen and Tronstad (1980). Here a similar wood species, spruce, was dried to 10% moisture content in 6.6 days using 0.89 kwh/kg of water extracted. Costs for the solar-absorption dryer were taken from Mueller Associates (1981) and are summarized in Table 6. The total installed system cost was $2,910,000. Table 7 is a comparison of the energy consumption and economics for the four drying systems.

The wood-fired boiler has a much higher capital cost than the oil boiler because of the handling and stoker system. The vapor-compression dehumidifer had the lowest capital cost of all. The energy costs of the vapor-compression dehumidifier and oil-fired boiler were about the same because both use expensive energy sources.

TABLE 5. *Drying time, energy consumption, and energy costs for a solar-absorption dehumidification kiln drying 2.54-cm-thick yellow poplar lumber.*

	January	April	July	October	Average
Drying time (days)	5.0	5.2	5.4	4.2	4.9
Energy consumption:					
Fan energy					
Cooling coil (kwh)	344	354	405	316	
Heating coil (kwh)	547	554	561	400	
Circulation (kwh)	328	339	350	271	
Total fan energy (kwh)	1,219	1,247	1,316	987	1,192
Pump energy					
Heating coil (kwh)	3	3	3	3	
Solar collectors (kwh)	1,448	1,714	1,877	1,260	
Absorption unit (kwh)	188	194	222	173	
Total pump energy (kwh)	1,639	1,911	2,103	1,435	1,772
Total parasitic energy (kwh)	2,858	3,158	3,419	2,422	2,964
Energy cost at 5¢ per kwh	$143	$158	$171	$121	$148
Specific energy consumption (kwh/kg)	0.119	0.131	0.142	0.101	0.123

The solar system had the lowest fuel cost of all. All the systems used about $700 in electrical energy just to operate the circulation fan in the kiln.

Even though the solar dryer saved about $41,000 on the 832,000 kWh of electrical energy, compared to the vapor-compression dehumidifier, it is doubtful if the solar system would be able to recover the capital cost during the life of the system. A simple payback time based on the data of Table 7 gives a value of about 65 years for the solar-absorption system versus the vapor-compression dehumidification system. However, if the cost of the solar components could be reduced, particularly the collectors, then the solar-absorption could probably become competitive economically to conventional drying systems.

CONCLUSIONS

The computer model indicated that a solar-absorption dehumidifier can dry 2.54-cm-thick yellow-poplar lumber at a rate equal to conventional steam kilns.

TABLE 6. *Solar-absorption dehumidifier system costs.*

Collector array	$300/m^2	Liquid storage	$448/m^3
Support structure	95/m^2	Electrical	110/m^2
Energy transport	140/m^2	General construction	45/m^2

TABLE 7. *Capital costs and yearly fuel costs for various types of lumber drying systems for drying 2,700 m³ (1,125,000 bd ft) of 2.54 cm yellow-poplar lumber.*

Cost	System			
	Wood-fired boiler	Oil-fired boiler	Vapor-compression dehumidifier	Solar-absorption dehumidifier
Initial	$146,000	$40,000	$25,000	$2,760,000
Base fuel	11,000	37,400	—	—
Electric fuel	724	724	48,200	6,600
Total energy	11,724	38,124	48,200	6,600

Kiln dry bulb and wet bulb temperature were kept fairly constant because of the hot and cold energy storage tanks. The absorption unit itself consumed little of the total electrical energy used by the complete solar system; the fans and other pumps were the main energy users. The solar-absorption drying system reduced the electrical energy consumption by 85% compared to a vapor-compression dehumidification system. Unfortunately, at the present time the overall economic advantages of the solar-absorption wood dryer are not attractive because of the large initial capital expenditure resulting mainly from the high cost of solar collectors. However, if the collector cost can be reduced (or if fossil fuel and electric energy costs become exorbitant), this type of dehumidification drying could become competitive with vapor-compression systems.

REFERENCES

ALLEN, R. W., AND F. H. MORSE. 1976. Optimization studies of solar absorption air conditioning systems. Report No. NSF/RANN/SE/GI39117/PR/76/2, National Science Foundation, Washington, D.C.

ANAND, D. K., R. W. ALLEN, AND B. KUMAR. 1982. Transient simulation of absorption machines. Trans. of ASME J. Solar Energy Eng. 104(3):197–203.

ANONYMOUS. 1976. Solaire® 36, 3-ton absorption chiller for solar air conditioning. Product Literature, Arkla Industries, Inc., Evansville, IN.

———. 1979. Air cooling and dehumidifying coils. ASHRAE Handbook-Equipment, ASHRAE, Atlanta, GA. Pp. 11–17.

———. 1980. Solartron vacuum-tube solar collector TC-100. Product Literature, General Electric Co., Philadelphia, PA.

AUER, W. W. 1980. Solar energy systems for agricultural and industrial process in drying. Drying '80, Vol. I. *In* Developments in drying. McGill University, Montreal. P. 280.

AUH, P. C. 1977. A survey of absorption cooling technology in solar applications. Report No. BNL-50704, Brookhaven National Laboratory, Upton, NY.

———. 1979. Development of hardware simulators for tests of solar cooling/heating subsystems and systems: Phase II—Unsteady state hardware simulation of residential absorption chiller. Brookhaven National Laboratory, Upton, NY.

BLINN, J. C., J. W. MITCHELL, AND J. A. DUFFIE. 1979. Modelling of transient performance of residential solar absorption air conditioning system. Proceedings of the 1979 International Solar Energy Congress.

BOGART, M. J. 1982. Lithium bromide absorption refrigeration—A calculator program. ASHRAE Journal 24(8):23–28.

BRAMHALL, G. 1976. Semi-empirical method to calculate kiln-schedule modification for some lumber species. Wood Sci. 8(4):213–222.

CINQUEMANI, V., J. R. OWENBY, AND R. G. BALDWIN. 1978. Input for solar systems. A report to Department of Energy for the National Climatic Center under Agreement No. E(49-26)-1041. 192 pp.

COMSTOCK, G. L. 1975. Energy requirements for drying—Lumber, veneer, particles. *In* Wood residue

as an energy source. Conference Proceedings of the Forest Products Research Society, September 3–5, Denver, CO. P. 8.

CURTIS, A. B. 1982. Economics of local and regional firewood markets. *In* Proceedings of the Fuelwood Management and Utilization Seminar, Michigan State University, November 1982. P. 36.

EGGEN, G., AND S. TRONSTAD. 1980. Dehumidification drying-conventional drying comparative tests on energy consumption. *In* Proceedings of the IUFRO V Conference—Wood Drying Papers, Oxford, England, April, 1980. P. 19.

GUERTIN, J. A., AND B. D. WOOD. 1980. Transient effects on the performance of a residential solar absorption chiller. Proceedings of the 1980 Annual Meeting AS/ISES, Phoenix, AZ. P. 186.

HELMER, W. A., P. Y. S. CHEN, H. N. ROSEN, AND S. W. WANG. 1980. A theoretical model for solar dehumidification drying of wood. Drying '80, Vol. II. *In* Proceedings of the Second International Symposium on Drying, McGill University, Montreal. Pp. 21–28.

———, ———, AND M. B. VAIDYA. 1982. A computer model to simulate solar and solar-dehumidification lumber drying. Trans. ASME J. Solar Eng. 104(3):182–186.

LIU, B. Y. H., AND R. C. JORDAN. 1977. Availability of solar energy for flat-plate solar heat collectors. *In* Applications of solar energy for heating and cooling of buildings, ASHRAE, Atlanta, GA. Pp. v1–v26.

LUNDE, P. J. 1980. Solar thermal engineering. John Wiley and Sons, New York, NY. P. 443.

MUELLER ASSOCIATES, INC. 1981. Solar energy system construction costs. Draft Report 81-183.

RASMUSSEN, E. F. 1961. Dry kiln operators manual. Agriculture Handbook No. 188, Forest Products Laboratory, USDA Forest Service, Madison, WI. P. 144.

ROSEN, H. N., P. Y. S. CHEN, AND W. A. HELMER. 1982. Solar and solar-dehumidification drying of lumber. *In* Proceedings of the 50th Anniversary of the Forestry Program at Stellenbosch University, Stellenbosch, Cape Town, South Africa. Pp. 9, 12.

NOMENCLATURE

A_c = surface area of cold heat storage tank, m^2
A_h = surface area of hot heat storage tank, m^2
A_l = top surface area of liquid solar collector, m^2
C_c = thermal capacitance of cold heat storage system, kJ/K
C_h = thermal capacitance of hot heat storage system, kJ/K
E = energy consumption, kJ
f_1 = function in equation (3)
f_2 = function in equation (4)
η = solar collector efficiency factor, dimensionless
Δh = height of water column pressure drop, m
I = solar insolation rate, W/m^2
$\dot{m}$ = mass flow rate, kg/s
q_c = heat loss rate from cold heat storage tank, kJ/s
q_{cool} = cooling capacity of absorption machine, kJ/s
q_d = heat transfer rate from dehumidifying coil, kJ/s
q_{gen} = heat transfer rate into the generator, kJ/s
q_h = heat loss rate from hot heat storage tank, kJ/s
q_l = rate of heat transfer collected in the liquid solar collector, kJ/s
T_a = ambient temperature, °C
T_c = condenser water inlet temperature, °C
T_{cs} = average cold storage fluid temperature, °C
T_g = generator temperature, °C
$T_{g,c}$ = generator temperature during cool-down, °C
$T_{g,h}$ = generator temperature during heat-up, °C
$T_{g,0}$ = initial generator temperature, °C

$T_{g,ss}$ = steady-state generator temperature, °C
T_{hs} = average hot storage fluid temperature, °C
T_i = solar collector inlet temperature, °C
T_{wb} = ambient wet bulb temperature, °C
U_c = overall heat loss coefficient for cold storage tank, $W/m^2 - °C$
U_h = overall heat loss coefficient for hot storage tank, $W/m^2 - °C$
U_l = overall heat loss coefficient for solar collector, $W/m^2 - °C$
t = time, s
t_0 = initial time, s
Δt = time increment, s
$(\tau\alpha)$ = solar transmittance absorptance product, dimensionless
τ_c = cooling time constant for absorption machine, s
τ_h = heating time constant for absorption machine, s
η = solar collector efficiency, dimensionless
η_m = motor efficiency, dimensionless
ρ = density of fluid, kg/m^3
ρ_w = density of water, kg/m^3